Presented at the 1998 American Control Conference, Session FA01, June 24-26, 1998
Philadelphia, PA

Optimal Filtering to Minimize the Elastic Behavior in Serial Link Manipulators

David P. Magee
Texas Instruments, Inc.
P.O. Box 655303, MS 8368
Dallas, TX 75265
magee@ti.com

Wayne J. Book
Georgia Institute of Technology
Mechanical Engineering Department
Atlanta, GA 30332-0405
wayne.book@me.gatech.edu

Abstract

This paper presents a new optimal filtering algorithm called the Optimal Arbitrary Time-delay (OAT) filter that has been designed to minimize the elastic behavior in serial link manipulators. However, as the analysis will show, the filtering algorithm can reduce the level of vibration in any system whose elastic motion can be modeled as a set of linear, ordinary differential equations with proportional damping. After analyzing some of the filter properties, experimental results demonstrate just how well the optimal filtering algorithm can minimize vibration.

1. Introduction

As task dimensions for manufacturing and assembly processes continue to get smaller, a larger portion of the overall task execution time is spent waiting for vibrations to settle. This inefficient use of time warrants better vibration suppression algorithms for the robots and mechanisms that perform these tasks. Nearly ten years ago, Singer and Seering [4] proposed an input shaping technique to cancel vibration generated by an input. Although other researchers had similar vibration suppression ideas [1,6], no other work in this area has seemed to spawn such a flurry of research. Advancements in digital computers might be part of the reason. Since their idea was founded on the impulse response of a second-order system, their method can be easily realized in a digital control system. However, other circumstances, such as improved efficiency in manufacturing environments, have also demanded better control systems that can properly compensate for elasticity in the manipulator system.

As a result, many researchers have focused on ways to reduce the level of vibration in elastic systems. This paper presents a new filtering algorithm that is derived from the linearized equations of motion for a serial link manipulator. The filtering algorithm essentially minimizes a cost function consisting of the elastic generalized coordinates and their velocities. Once the closed form solution is presented for the optimal filtering coefficients, some filter properties are given. The paper concludes with experimental results using a two-link, elastic manipulator to demonstrate the vibration suppression capabilities of the new filtering algorithm.

For the terms in any filtering algorithm to have physical significance, they must be related to the parameters describing the system. More often than not, the connection is made through a mathematical model. The next section provides a summary of the dynamic equations of motion for serial link manipulators. To fully appreciate the complexity of deriving such a model, see [3].

2. Modeling

This section begins with a general, nonlinear model for a serial link manipulator and then presents an approximation of the model for configurations near a nominal operating point. This linear set of ordinary differential equations becomes the mathematical foundation for the derivation of the optimal filtering algorithm. The equations are then transformed into state space form to simplify the analysis and to utilize the unique properties of the state transition matrix.

2.1 Linearized Equations of Motion

The dynamic equations of motion for a serial link manipulator can be expressed in matrix notation as

$$M(q)\ddot{q} + C(q,\dot{q})\dot{q} + D\dot{q} + Kq + g(q) = B\tau \qquad (1)$$

where $M(q)$ is the inertia matrix, $C(q,\dot{q})$ is the Coriolis and centrifugal matrix, D is the damping matrix, K is the stiffness matrix, $g(q)$ is the gravity vector, B is the input influence matrix, τ is the input force/torque vector and q is a vector of rigid-body and elastic generalized coordinates. This set of equations is nonlinear and is a function of the generalized position and velocity vectors. However, by carefully analyzing each term, the matrix equation can actually be divided into two matrix equations: one for the rigid-body generalized coordinates and one for the elastic generalized coordinates.

For most systems, an exact model usually does not exist or is not feasible for real time implementation. In these situations, a linear approximation of the system is developed for an arbitrary configuration. By defining a generalized variable $\hat{q}$ to represent the incremental motion from a nominal operating point $\bar{q}$, the linearized dynamic equations of motion for a serial link manipulator can be derived [3]. Although the step by step details are omitted from this paper, the linear dynamic equations of motion describing the elastic system behavior can be written as

$$\overline{M}_e\ddot{\hat{q}}_e + D_e\dot{\hat{q}}_e + K_e\hat{q}_e = -M_{re}^T(\overline{q})M_r^{-1}(\overline{q})\hat{\tau} \quad (2)$$

where r and e denote the rigid-body and elastic coordinates, respectively.

This equation is the focal point for the optimal filtering algorithm derivation in this paper. The matrix equation is first written in state space form to reduce the number of terms. Then an optimal filtering algorithm is proposed that minimizes the level of vibration during commanded motions of the system.

2.2 State Space Form

The model for the elastic motion in Equation (2) can be written in the state space form

$$\dot{\hat{x}}_e = \overline{A}_e\hat{x}_e + \overline{B}_e\hat{\tau} \quad (3)$$

where

$$\overline{A}_e = \begin{bmatrix} 0_{m\times m} & I_{m\times m} \\ -\overline{M}_e^{-1}K_e & -\overline{M}_e^{-1}D_e \end{bmatrix} \quad (4)$$

and

$$\overline{B}_e = \begin{bmatrix} 0_{m\times n} \\ -\overline{M}_e^{-1}M_{re}^T(\overline{q})M_r^{-1}(\overline{q}) \end{bmatrix} \quad (5)$$

and m and n are the total number of elastic and rigid-body coordinates. The state vector consists of the elastic coordinates and their velocities so that $\hat{x}_e = \begin{bmatrix}\hat{q}_e & \dot{\hat{q}}_e\end{bmatrix}^T$.

Since the equations are linear, the solution can be expressed in terms of the state transition matrix for the elastic dynamics, $\phi_e(t,t_0)$, as

$$\hat{x}_e(t) = \phi_e(t,t_0)\hat{x}_e(t_0) + \int_{t_0}^{t}\phi_e(t,\tau)\overline{B}_e\hat{\tau}(\tau)d\tau . \quad (6)$$

Notice that when the input is zero, the state transition matrix $\phi_e(t_1,t_0)$ maps the elastic states of the system from any time t_0 to any future time t_1.

3. Optimization

Since the state transition matrix can predict the behavior of the elastic system, a filtering algorithm is proposed as a way to modify the input so that the elastic system response is minimized. This section presents the general form for this filter and then provides a method for determining the optimal filter coefficients. Conditions are also given to guarantee a minimum elastic response.

3.1 OAT Filter Form

Given a relationship between the input and the elastic system response, a filter can be designed to generate a desired elastic response. Each input filter contains an arbitrary time-delay value and can be written in the general form

$$f_i(t) = \sum_{j=0}^{p_i} f_{ij}\cdot\delta(t - j\cdot T_i) \quad (7)$$

with $f_{i0} = 1$ and $1 \le i \le n$. The term f_{ij} is the j^{th} coefficient for the i^{th} input filter, $\delta(t)$ is the Dirac delta function, T_i is an arbitrary time-delay value for the i^{th} input filter, and $p_i + 1$ is the number of filter coefficients in the i^{th} input filter. Notice that the coefficients for each filter have been normalized so that the first coefficient is one. This normalization is arbitrary but simplifies the solution process for the optimal filter coefficients. After solving for the optimal coefficients, they can be re-normalized to given the filter some preferred characteristics.

3.2 Cost Function

The cost function, $J(t)$, for the design of this particular filtering algorithm is a weighted sum of the elastic coordinates and their velocities. It can be written as

$$J(t) = \tfrac{1}{2}\hat{x}_e^T(t)\,W\,\hat{x}_e(t) \quad (8)$$

where

$$W = \begin{bmatrix} W_1 & 0_{m\times m} \\ 0_{m\times m} & W_2 \end{bmatrix} \quad (9)$$

and W_1 and W_2 are positive definite, symmetric weighting matrices for the position and velocity, respectively. Notice that this particular cost function just evaluates the states at each time instant and does not contain an integral term involving the states or the input.

By convolving each input in Equation (6) with its own filter, the cost function becomes an explicit function of the unknown filter coefficients. Since the number of filter coefficients and the time-delay values are not necessarily the same for each filter, the cost function can only be minimized after the last input is given (i.e. $t > p_k\cdot T_k$). The cost function is also a function of the initial conditions. However, they do not provide any additional information about the system behavior so they are set to zero [2].

To study a particular input's effect on the elastic response of the system, an impulse is given as the i^{th} input and all of the other inputs are set to zero. With an impulse input and a linear system, the solution for the optimal filter coefficients extends to a general input because any signal can be written as a scaled sequence of impulses separated by an infinitesimal amount of time.

With these simplifications, the cost function can be written as

$$J(t) = \tfrac{1}{2}\left(\phi_e(t,0)\overline{B}_{e_{*i}} + \Phi_i(t)\hat{f}_i\right)^T W\left(\phi_e(t,0)\overline{B}_{e_{*i}} + \Phi_i(t)\hat{f}_i\right) \quad (10)$$

where

$\Phi_i(t) = \begin{bmatrix}\phi_e(t,T_i)\overline{B}_{e_{*i}} & \cdots & \phi_e(t,p_i\cdot T_i)\overline{B}_{e_{*i}}\end{bmatrix}$, $\overline{B}_{e_{*i}}$ is the i^{th} column of the $\overline{B}_e$ matrix and $\hat{f}_i$ is a vector of unknown filter coefficients for the i^{th} input filter. This matrix form

provides a compact notation for the optimization procedure in the next section.

3.3 Conditions for a Minimum

From parameter optimization, the two necessary and sufficient conditions for the cost function to have a minimum are

$$\frac{\partial J}{\partial \hat{f}_i} = 0_{1\times p_i} \tag{11}$$

and

$$\frac{\partial^2 J}{\partial \hat{f}_i^2} \geq 0_{p_i\times p_i}. \tag{12}$$

After performing the operation specified by the first condition, the roots of the resulting equation are the critical points of the cost function. If the second condition at a particular critical point is true, then the cost function is a minimum and the critical point is an optimal value. Evaluating the cost function according to the first condition and solving for the unknown filter coefficients, $\hat{f}_i$, yields

$$\hat{f}_i = -\left[\Phi_i^T(t) W \Phi_i(t)\right]^{-1} \Phi_i^T(t)\, W\, \phi_e(t,0) \overline{B}_{\psi_{ei}}. \tag{13}$$

These filter coefficients are the critical points of the cost function and are potentially the optimal values. Applying the second condition generates the equation

$$\Phi_i^T(t) W \Phi_i(t) \geq 0_{p_i\times p_i} \tag{14}$$

since the weighting matrix is symmetric.

3.4 OAT Filter Coefficients

It is impossible to say whether or not Equation (14) is true for all systems. However, if conditions are placed on the $\Phi_i(t)$ matrix, then a solution can be guaranteed. Using results from linear algebra [5], the matrix $\Phi_i^T(t) W \Phi_i(t)$ is positive definite when the matrix $\sqrt{W}\Phi_i(t)$ has linearly independent columns. If the matrix $\Phi_i^T(t) W \Phi_i(t)$ is positive definite, then Equation (14) is satisfied. The positive definite property of this matrix also ensures that the inverse in Equation (13) can always be computed.

The optimal filter coefficients given by Equation (13) guarantee that the cost function given by Equation (8) is minimized. Since each filter can have its own arbitrary time-delay value T_i, this optimal filter has been named the OAT (Optimal Arbitrary Time-delay) filter. This filtering algorithm, and the related analysis, is being patented by the Georgia Institute of Technology and commercial use of these ideas may require a license.

4. Properties of the OAT Filter

Now that a filtering algorithm has been derived to minimize the elastic system response, the OAT filter will be analyzed for one mode of vibration. This section also evaluates the zeros of the filter and shows that the filtering algorithm achieves pole-zero cancellation regardless of the time-delay value.

4.1 OAT Filter for One Mode of Vibration

A single mode of vibration can be described by the second-order, ordinary differential equation

$$\ddot{\hat{q}}_e + 2\zeta\omega_n \dot{\hat{q}}_e + \omega_n^2 \hat{q}_e = \frac{1}{\overline{m}_e}\hat{\tau} \tag{15}$$

where ζ is the damping ratio, ω_n is the natural frequency of the undamped system and $\overline{m}_e$ is the effective inertia of the elastic system. The corresponding OAT filter that minimizes this elastic response is

$$\begin{aligned}\hat{f}_1(t) = \delta(t) - 2\cos(\omega_d T_1) e^{-\zeta\omega_n T_1}\delta(t-T_1) \\ + e^{-2\zeta\omega_n T_1}\delta(t-2\cdot T_1)\end{aligned} \tag{16}$$

where $\delta(t)$ is the Dirac delta function, ω_d is the damped natural frequency of the system and T_1 is an arbitrary time-delay value.

4.2 Zeros of the OAT Filter

The Laplace transform can convert the OAT filter representation from the time domain into the complex s-domain so that the zeros can be determined. Taking the Laplace transform of Equation (16) produces

$$\begin{aligned}\hat{F}_1(s) = 1 - 2\cos(\omega_d T_1) e^{-\zeta\omega_n T_1} e^{-sT_1} \\ + e^{-2\zeta\omega_n T_1} e^{-s2T_1}\end{aligned} \tag{17}$$

which has zeros located at

$$s = -\zeta\omega_n \pm j\left(\omega_d + \frac{2n\pi}{T_1}\right) \tag{18}$$

for $n = 0, \pm 1, \ldots, \pm\infty$.

This equation shows that the OAT filter places a set of zeros at the pole locations of the single mode of vibration. And, pole-zero cancellation occurs regardless of the time-delay value. In fact, by cleverly choosing the time-delay value, two lightly damped modes of vibration can be canceled with just one OAT filter.

The pole-zero cancellation characteristic of the OAT filter applies when a system has multiple modes of vibration as well. To minimize the vibration in this system, the overall OAT filter is just the convolution of OAT filters for each mode of vibration [3]. Verification of this fact is left as an exercise for the reader.

5. Robustness

The analysis up to this point has assumed that the dynamic model of the system is exact. However, for a real system, this assumption is seldom true. Therefore, this section investigates the robustness of the OAT filtering algorithm to uncertainty in natural frequency, damping ratio and time-delay quantization. By adjusting the time-delay value, different levels of robustness can be achieved.

5.1 Vibration Error Expression

To measure the level of residual vibration resulting from parameter uncertainty and time-delay quantization, a VE (Vibration Error) expression will be defined to quantify the results. The VE is written as a magnitude ratio of an impulse response and a filtered impulse response for a second-order system. The second-order system in this analysis is simply the model for one mode of vibration like Equation (15). Mathematically, the VE can be written as

$$VE = \frac{|h_f(t)|}{|h(t)|} \quad \text{for} \quad t \geq p_1 \cdot T_1 \tag{19}$$

where $h_f(t)$ is the filtered impulse response and $h(t)$ is the impulse response. This error expression can be interpreted as a ratio of the exponential envelopes used to represent the respective response of a second-order system.

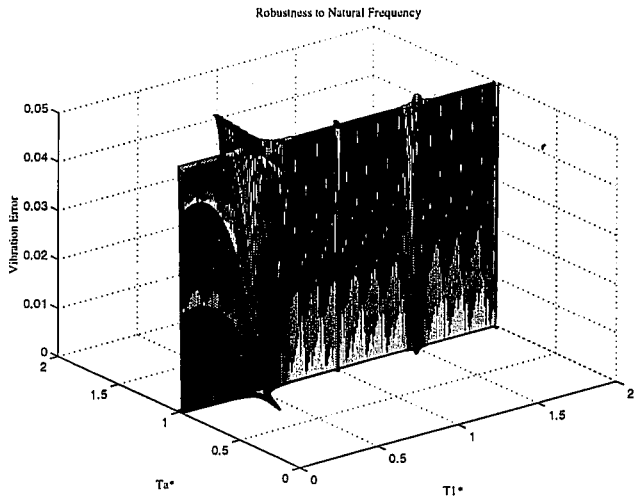

Figure 1. Robustness to Natural Frequency

Since the VE expression is a function of the modeled and actual system parameters, the robustness of the filtering algorithm can be determined by varying a particular system parameter and plotting the resulting VE. To generalize the results, the VE expression will be normalized with respect to the particular parameters in question. Since even the normalized form is still a function of the damping ratio, a value of $\zeta = 0.1$ will be used.

5.2 Robustness to Natural Frequency

The first occurrence of parameter uncertainty is when the modeled natural frequency, ω_n, differs from the actual natural frequency, ω_a, of the elastic system. Using two normalized ratios $T_1^* = \frac{T_1}{T_n}$ and $T_a^* = \frac{T_a}{T_n}$ (where $T_n = \frac{2\pi}{\omega_n}$ and $T_a = \frac{2\pi}{\omega_a}$), the VE expression can be plotted as a function of these two independent variables.

Figure 1 shows a plot of the VE over the ranges $0.01 \leq T_1^* \leq 2$ and $0.01 \leq T_a^* \leq 2$ with a 5% upper bound on the error values. Notice that a robustness trench exists along the line $T_a^* \approx 1$. This result makes intuitive sense because in the ideal modeling scenario, $T_n = T_a$. A contour plot of the three-dimensional surface has also been drawn to give the reader a feel for the size of the robustness regions.

Several regions also exist along the line where there is improved robustness to natural frequency. For example, near the point $T_1^* \approx 0.5$ and $T_a^* \approx 1$, the OAT filtering algorithm places two sets of zeros at the pole locations of the elastic system. Therefore, multiple zeros at a given set of pole locations in the complex s-domain produce a more robust filtering algorithm.

The plot of robustness to uncertainty in damping ratio for the OAT filtering algorithm is very similar in shape to the uncertainty in natural frequency plot. However, the regions are much larger indicating that the filtering algorithm is not very sensitive to this particular parameter.

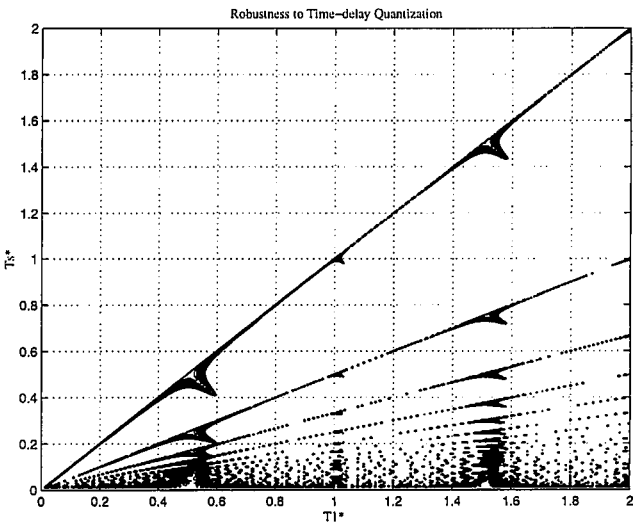

Figure 2. Robustness to Time-delay Quantization

5.3 Robustness to Time-delay Quantization

The last demonstration of robustness is when the time-delay value, T_1, is quantized. Using two normalized ratios T_1^* and $T_s^* = \frac{T_s}{T_n}$ (where T_s is the sampling period of the control system), the VE error expression can be plotted as a function of these two independent variables.

Figure 2 shows a plot of the VE over the ranges $0.01 \leq T_1^* \leq 2$ and $0.01 \leq T_s^* \leq 2$ with a 5% upper bound on the error values. Only a contour plot has been drawn for this example to simplify the figure. Notice that there are many discrete regions in the VE contour plot where the OAT filtering algorithm is robust to time-delay quantization. In fact, as the normalized time T_s^* decreases, the number of robustness regions increases. However, the

discrete regions of robustness for small values of T_s^* suggest that the time-delay value T_1 should be an integer multiple of the sampling period of the control system.

Regions of improved robustness for the OAT filtering algorithm also occur with respect to time-delay quantization. For example, regions where $T_1^* \approx 0.5$ correspond to the case when two sets of filter zeros are located at the elastic poles of the system. Another interesting observation is that there are no robustness regions above the line $T_s^* = T_1^*$, which means that the time-delay value cannot be shorter than the sampling period of the control system.

6. Experimental Results

Now that the OAT filter characteristics have been presented, the algorithm will be incorporated into a feedback control system to minimize the vibration in a two link, elastic manipulator named RALF [3]. The desired trajectory for the tip of the manipulator is a square. To measure the tip response of the manipulator, a landmark tracking system records the position of retro-reflective material attached to RALF's tip. The experimental results will demonstrate the filtering algorithm's effectiveness in reducing the level of vibration due to structural as well as base compliance.

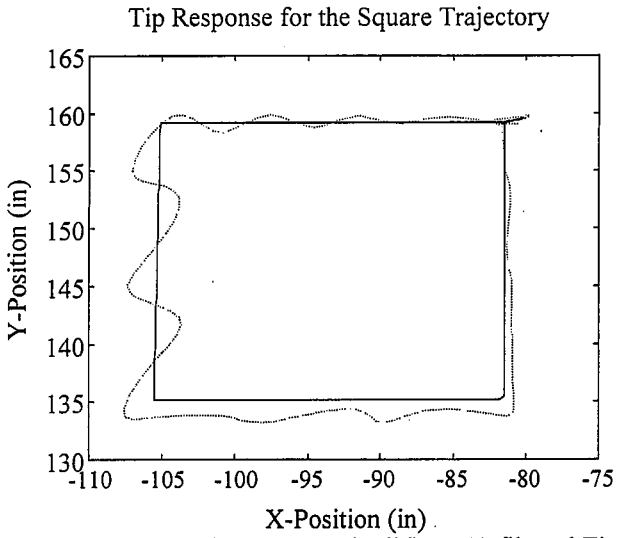

Figure 3. Desired Tip Response (Solid) vs. Unfiltered Tip Response (Dashed)

6.1 Square Trajectory

The desired trajectory for this set of experiments is a square consisting of 24" sides. With a desired tip speed of 30"/sec, RALF traverses the path in 3.2 seconds. Figure 3 shows the desired tip trajectory and the motion of the manipulator tip. The straight-line motion near the coordinates (-80,160) is the tip of the manipulator moving into the field of view of the landmark tracking system and to the start point of the trajectory. The manipulator is commanded to hold at the start point for one second and then follow the square in a clockwise direction. After completing the square, the manipulator is again commanded to hold at the start point for one second and then move back to the home position along the same line.

The vibration of the manipulator is visually obvious in this figure. However, to quantify the level of vibration, the average and maximum position error in the x and y directions will be calculated. For the unfiltered response, the average x-position error is 1.4" and the maximum x-position error is 5.0". In the y-direction, the average position error is 1.4" and the maximum position error is 5.9".

6.2 Filtering for Base and Structural Resonances

The vibration in the tip response during the square trajectory is due to the structural compliance of each link in RALF and to a crack in the manipulator base. To demonstrate the versatility of the OAT filtering algorithm, a filter was designed for each mode of vibration. To cancel the mode of vibration associated with the first structural resonance of RALF, an OAT filter was designed for a natural frequency of 4.9 Hz, a damping ratio of 0.07 and a time-delay value of 0.04 seconds. The filter was positioned inside a joint PID feedback control loop to shape the voltage command to each servo-valve on each actuator of the manipulator.

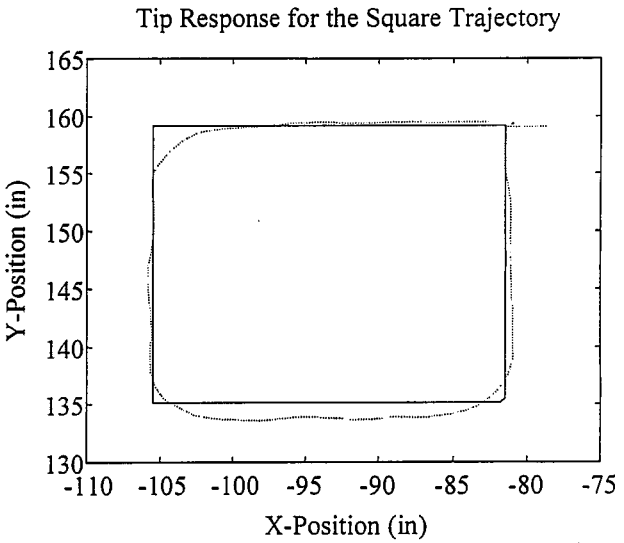

Figure 4. Desired Tip Response (Solid) vs. Filtered Tip Response (Dashed)

To compensate for the crack in the base, the resonant behavior had to first be characterized. After analyzing several frequency responses, an OAT filter was designed for a natural frequency of 2.7 Hz and a damping ratio of 0.02. A time-delay value of 0.2 seconds representing the most robust region of the OAT filtering algorithm was chosen for this filter because of the uncertainty in the system parameter values. As a result, the

filter could not be located inside the feedback control loop because of stability reasons. Therefore, the filter algorithm was implemented as a pre-feedback filter and located just before the feedback control system to shape the desired joint trajectory.

Figure 4 shows the desired and actual tip response of the manipulator after filtering for the two modes of vibration. The level of vibration has been reduced significantly and is visually apparent after comparing Figures 3 and 4. To quantify the results, the average and maximum position error calculations were computed. In the x-direction, the average error was 2.7" and the maximum error was 8.7". In the y-direction, the average error was 2.8" and the maximum error was 9.3".

These errors are actually larger than the results from the previous experiment. The reason is related to the long time-delay value used in the filter to minimize the vibration level coming from the crack in the base. As a result, these position error calculations do not really provide any information about the vibration suppression ability of the OAT filtering algorithm. However, if the time-delay value for the base resonance is shortened, the tracking performance of the manipulator improves [3].

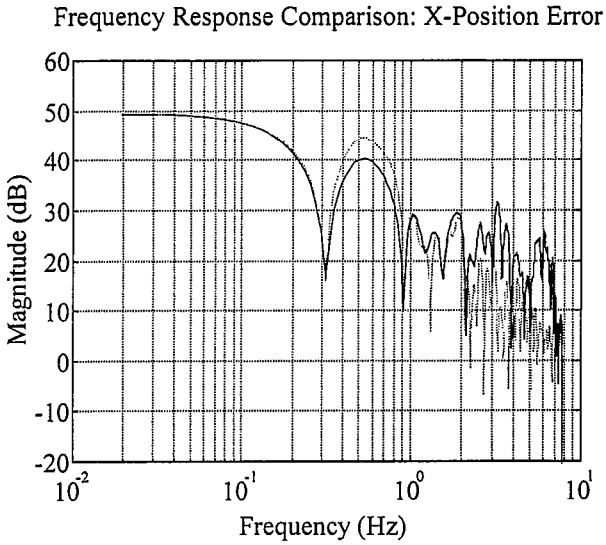

Figure 5. Frequency Response Comparison: Unfiltered Response (Solid) vs. Filtered Response (Dashed)

To quantify the vibration cancellation ability of the OAT filtering algorithm, the responses must be transformed into the frequency domain. Figure 5 shows the frequency response of x-position error for the unfiltered and the filtered experiments. At the base frequency (2.7 Hz), the vibration magnitude was reduced by 9.6 dB. At the first structural frequency (4.9 Hz), the vibration magnitude was reduced by 6.9 dB. However, the improved robustness of the OAT filter designed for the 2.7 Hz mode produced magnitude reductions of up to 20 dB at other frequency values.

The frequency response of the y-position error reveals the same level of vibration suppression capability for the OAT filtering algorithm. At the base frequency, the magnitude of vibration was reduced by 7.6 dB. For the first structural frequency, the magnitude of vibration was reduced by 16.1 dB. As in the frequency response for the x-position error, magnitude reductions also appear at frequencies near the base mode of vibration. The vibration magnitude is nearly 25 dB lower in this region.

7. Conclusions

This paper presented an OAT (Optimal Arbitrary Time-delay) filtering algorithm that can minimize the level of vibration in any system whose elastic dynamics can be approximated by a set of linear, ordinary differential equations. The variable time-delay parameter makes it ideal for discrete-time implementations, such as a digital control system, without loss of filter performance. For systems with large amounts of parameter uncertainty, the time-delay value can also be chosen to improve robustness.

The effectiveness of the filtering algorithm to minimize vibration was then demonstrated using a two link manipulator. For the square trajectory in the experiments, the level of vibration was reduced by at least 7 dB at the designated frequencies and by nearly 25 dB in other frequency regions. This level of vibration suppression makes the OAT filtering algorithm a viable tool for overcoming the limitations generated by compliance in many of the robots and mechanisms found in today's manufacturing environments.

8. References

1. Calvert, J.F. and Gimpel, D.J., "Method and Apparatus for Control of System Output in Response to System Input," Patent No.2,801,351, United States of America, July 30, 1957.
2. Goodwin, G.C. and Sin, K.S. *Adaptive Filtering Prediction and Control*, Prentice-Hall, Inc., Englewood Cliffs, NJ, 1984.
3. Magee, D.P., *Optimal Arbitrary Time-delay Filtering to Minimize Vibration in Elastic Manipulator Systems*, Ph.D. Thesis, Georgia Institute of Technology, August 1996.
4. Singer, N.C. and Seering, W.P., "Preshaping Command Inputs to Reduce System Vibration," *ASME Journal of Dynamic Systems, Measurement and Control*, Vol.112, No.1, March 1990, pp.76-82.
5. Strang, G., *Linear Algebra and Its Applications*, Third Edition, Harcourt Brace Jovanovich, Publishers, San Diego, CA, 1988.
6. Tallman, G.H. and Smith, O.J.M., "Analog Study of Dead-Beat Posicast Control," *IRE Transactions on Automatic Control*, Vol.PGAC, No.4, March 1958, pp.14-21.